

A bivariate Normal Inverse Gaussian process with stochastic delay: efficient simulations and applications to energy markets

Matteo Gardini* Piergiacomo Sabino[†] Emanuela Sasso[‡]

October 15, 2021

Abstract

Using the concept of self-decomposable subordinators introduced in Gardini et al. [11], we build a new bivariate Normal Inverse Gaussian process that can capture stochastic delays. In addition, we also develop a novel path simulation scheme that relies on the mathematical connection between self-decomposable Inverse Gaussian laws and Lévy-driven Ornstein-Uhlenbeck processes with Inverse Gaussian stationary distribution. We show that our approach provides an improvement to the existing simulation scheme detailed in Zhang and Zhang [23] because it does not rely on an acceptance-rejection method.

Eventually, these results are applied to the modelling of energy markets and to the pricing of spread options using the proposed Monte Carlo scheme and Fourier techniques.

1 Introduction and preliminaries

The Black and Scholes [5] model is probably the most popular stochastic model used to describe the dynamics of financial indices. Even though it is well-known that it is not able to capture many stylized facts, its simplicity and its flexibility often make it the standard choice for many financial applications. In the univariate setting several models have been proposed to overcome its limits, relying, for example, on

*Department of Mathematics, University of Genoa, Via Dodecaneso 16146, Genoa, Italy, email gardini@dima.unige.it

[†]Quantitative Modelling E.ON SE Brüsseler Platz 1, 45131 Essen, Germany, email piergiacomo.sabino@eon.com

[‡]Department of Mathematics, University of Genoa, Via Dodecaneso 16146, Genoa, Italy, email sasso@dima.unige.it

more general Lévy processes. However, in a multi-market setting, the Black-Scholes model is still a milestone due to the fact that alternatives can be less mathematically tractable and their calibration can be computationally demanding. An attempt to combine tractability and simple calibration in a multivariate framework has been proposed by Semeraro [20] in the context of Variance Gamma (VG) processes, introduced by Madan and Seneta [15] and extended to Normal Inverse Gaussian (NIG) processes, introduced by Barndorff-Nielsen [3], in Luciano and Semeraro [14]. Each marginal of the multivariate process is built via Brownian subordination: the resulting subordinator is the sum of an independent subordinator and a subordinator shared by all the components, both mutually independent. Therefore, the construction has a nice financial interpretation in terms of idiosyncratic and systematic risks. An alternative approach to construct multidimensional Lévy processes including VG and NIG processes, has been proposed by Ballotta and Bonfiglioli [1] sharing the same logic of idiosyncratic and systematic risks. Such models are able to capture some empirical facts such as discontinuities in price trajectories, volatility smiles and non-normality in log-returns, whereas the joint dependence is driven by the common systematic component.

On the other hand, the impact of new information in one market might require some time to be propagated onto dependent markets therefore, the aforementioned models cannot replicate any *stochastic delay* or any *synaptic risk* as named in Cufaro Petroni and Sabino [9]. Indeed, it is not so rare to observe that the impact on other related markets occurs after a stochastic time delay. Nowadays, a clear example is offered by the recent pandemic disease of Covid-19: as one can see in Figure 1, first blown cases appeared at the beginning of January 2020 in China leading to a big downward jump in Shanghai's index after a flat period due to Chinese New Year celebrations and subsequently the virus spread all over the world. Italy registered first cases at the end of February, Brazil at the beginning of March leading to a general drop in the whole world economy.

Recently in Gardini et al. [11] we have shown how the notion of self-decomposability (*sd*) can be used to describe stochastic delays and to introduce synaptic risk in financial models. We recall that the law of a *rv* X is said to be *sd* (see Sato [19] and Cufaro Petroni [8]) if for every $a \in (0, 1)$ its characteristic function (*chf*) $\phi(u)$ can be represented as

$$\phi_X(u) = \phi_X(au) \chi_a(u). \quad (1)$$

with $\chi_a(u)$ also a *chf*. It means that we can always find two independent *rv*'s Y (with the same law of X) and Z_a such that, in distribution

$$X \stackrel{d}{=} aY + Z_a$$

where of course, $\chi_a(u)$ is the *chf* of Z_a (hereafter called the a -remainder of the law of X) whose law is infinitely divisible (*id*) but not in general *sd* (see Sato [19]).

Based on these facts, in Gardini et al. [11] we have introduced what we name *sd-subordinators* that are the building blocks for the construction of correlated Lévy

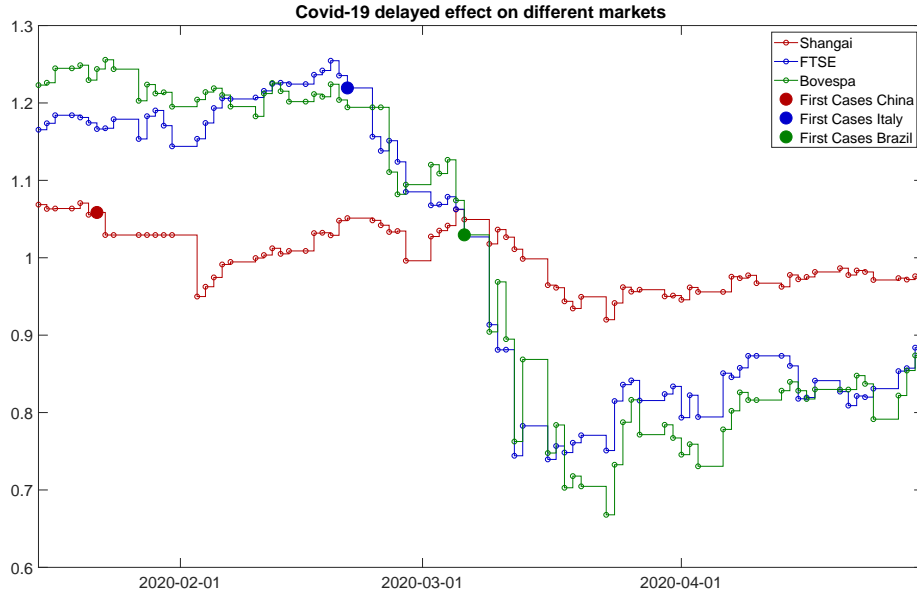


Figure 1: Impact of Covid-19 disease in some markets world wide.

processes. In analogy to *sd* laws, such subordinators $H_1(t), H_2(t)$ are defined as follows

$$H_2(t) = aH_1(t) + Z_a(t) \quad (2)$$

where $H_2(t)$ and $Z_a(t)$ are independent processes. The last equation is mathematically well-posed and has a clear interpretation: the stochastic time processes $H_1(t), H_2(t)$ “run together” with a stochastic delay $Z_a(t)$ that is controlled by a that simply plays the role of the instantaneous correlation between $H_1(t)$ and $H_2(t)$. When a tends to 1 then $H_1(t)$ and $H_2(t)$ become essentially indistinguishable. By subordinating Brownian motions (BM) with such subordinators we construct a class of dependent processes that are at least marginally Lévy. This means that we can extend the approaches of Semeraro [20], Luciano and Semeraro [14] and Ballotta and Bonfiglioli [1] to cover stochastic delays while keeping mathematical tractability, easy calibration and clear financial interpretation.

This study can be considered the sequel of Gardini et al. [11], where now our main focus is on bivariate *sd* Inverse Gaussian (IG) subordinators and on the construction of bivariate dependent NIG processes. The first contribution of this work is the derivation of closed form formulas for the linear correlation and the *chf* of the last processes. These results are instrumental for the calibration and the pricing of derivative contracts. The pricing of complex derivative contracts is often accomplished via Monte Carlo (MC) simulations. To this end, a second contribution of this study consists of a novel and efficient algorithm to generate the a -remainder of IG laws and therefore to simulate the skeleton of $Z_a(t)$, of the *sd* IG subordinators and of the bivariate NIG processes. As already observed among others in Taufer and Leonenko [21], Sabino [18] and Cufaro Petroni and Sabino [10], the transition

law between t and $t + \Delta t$ of a Lévy-driven Ornstein-Uhlenbeck (OU) $X(t)$ having a certain stationary law coincides with that of the a -remainder of such a law by setting $a = e^{-\lambda\Delta t}$ where λ is the mean-reversion rate of $X(t)$. Hence, the simulation of the a -remainder of a IG law is equivalent to the simulation of the skeleton of a IG-OU process, this last one having been illustrated in Zhang and Zhang [23]. We show that our proposal is more efficient than that of Zhang and Zhang [23], because it does not rely on acceptance-rejection methods. Note that being $Z_a(t)$ a Lévy process, its simulation requires the same a at all times t while instead $a = e^{-\lambda\Delta t}$ depends on the time step Δt .

Finally, we illustrate the applicability of the proposed bivariate sd -NIG processes to energy markets and in particular to the pricing of spread options via MC simulations and Fourier techniques.

The article is organized as follow: Section 2 introduces sd -NIG processes and their mathematical properties. In Section 3 we describe the method to simulate $Z_a(t)$ and hence $H_1(t), H_2(t)$ defined in Equation (2). In Section 4 we apply the models described in Section 2 to power and gas forward markets and to the pricing of spread options with MC and Fourier Techniques. Section 5 concludes the paper with an overview of future inquiries and possible further applications.

2 Self decomposable NIG process

The NIG process is constructed via the subordination of a BM with an IG process. On the other hand, there are different characterizations of the *pdf* of an IG law: we denote the notation using the parameter-setting (μ, λ) , adopted for instance in Cont and Tankov [7], with $IG_T(\mu, \lambda)$: within this setting $\mu > 0$ is the mean and $\lambda > 0$ is the shape parameter. On the other side, we refer to the original notation in Barndorff-Nielsen [2] with $IG_B(a, b)$: in this case $a > 0$ and $b > 0$ describe the scale and the shape of the distribution, respectively. In Appendix A we give some details on how to switch from one to the other. In general, the IG_B notation is convenient to analyze sums of IG *rv*'s, whereas IG_T is more convenient to work with expectations and *chf*.

Semeraro [20], Luciano and Semeraro [14] and Ballotta and Bonfiglioli [1] proposed a simple technique to introduce dependence between Lévy processes: given three Lévy independent processes $X_1(t)$, $X_2(t)$ and $Z(t)$ and $a_1, a_2 \in \mathbb{R}$ one can set:

$$\begin{aligned} Y_1(t) &= X_1(t) + a_1 Z(t) \\ Y_2(t) &= X_2(t) + a_2 Z(t) \end{aligned}$$

The processes $Y_1(t)$ and $Y_2(t)$ are clearly dependent, because of the common process $Z(t)$. This idea can be applied to different types of processes, included subordinators. The economic interpretation is clear: $Z(t)$ represents the *systematic*

risk whereas $X_j(t)$ models the *idiosyncratic risk*. Of course, this simple construction can be applied to obtain multivariate VG and NIG processes. Nevertheless, as mentioned in the introduction, these settings cannot cover stochastic-delay and what we call *synaptic risk*. In Gardini et al. [11] we detailed on the construction of bivariate *sd*-VG processes, whereas in this sequel we focus on the bivariate version of *sd*-NIG processes. In a nutshell, our approach consists of replacing the common and marginal-specific subordinators of Semeraro [20], Luciano and Semeraro [14] and Ballotta and Bonfiglioli [1] with *sd*-subordinators defined in (2).

2.1 Semeraro *sd*-NIG model

In this subsection we illustrate the steps required to extend the model proposed by Semeraro [20] in order to cope with stochastic delay relying on the *sd* subordinators of Equation (2).

Let $I_j(t)$ $j = 1, 2$ be independent subordinators, and $H_1(t)$, $H_2(t)$ be *sd* subordinators defined in (2), independent of $I_j(t)$. Define the subordinator $G_j(t)$

$$G_j(t) = I_j(t) + \alpha_j H_j(t), \quad j = 1, 2 \quad (3)$$

with $\alpha_j \in \mathbb{R}^+$. Let now be $\mu_j \in \mathbb{R}$, $\sigma_j \in \mathbb{R}^+$ and $W_j(t)$ standard independent BM's, we define the subordinated BM $Y_j(t)$ as:

$$Y_j(t) = \mu_j G_j(t) + \sigma_j W_j(G_j(t)), \quad j = 1, 2. \quad (4)$$

We remark that when a in (2) tends to 1 there is no time delay and the synaptic risk coincides with the systematic risk as in the original approach of Semeraro [20].

A bivariate NIG process with IG *sd*-subordinators can be defined starting from (3) in the following way. Let be $\alpha_j = \gamma_j^2$ and let $I_j(t)$ and $H_j(t)$ be distributed as follows:

$$\begin{aligned} I_j(t) &\sim IG_T \left(\frac{A_j \gamma_j t}{B}, A_j^2 t^2 \right) \\ H_j(t) &\sim IG_T \left(\frac{At}{B}, A^2 t^2 \right) \end{aligned} \quad (5)$$

and hence we get:

$$G_j(t) \sim IG_T \left(\frac{(A_j + A\gamma_j) \gamma_j t}{B}, (A_j + A\gamma_j)^2 t^2 \right).$$

Since $G(t)$ is a stochastic time, it is customary to require that $\mathbb{E}[G_j(t)] = t$: this condition can be easily fulfilled by imposing:

$$A_j + A\gamma_j = \frac{B}{\gamma_j}.$$

Consequently, denoting with k_j the variance of the subordinator $G(t)$ at time $t = 1$, we have that:

$$k_j := \text{Var}[G_j(1)] = \frac{1}{(A_j + A\gamma_j)^2} = \frac{\gamma_j^2}{B^2}.$$

As observed in Luciano and Semeraro [14], assuming $B = 1$ is not restrictive: hence $k_j = \gamma_j^2$ and then $k_j = \alpha_j$. After simple calculations, one can find that the expression of the (instantaneous) linear correlation coefficient at time t of the process $\mathbf{Y}(t) = (Y_1(t), Y_2(t))$ is:

$$\rho_{(Y_1(t), Y_2(t))} = \frac{\mu_1 \mu_2 \alpha_1 \alpha_2 a A}{\sqrt{\sigma_1^2 + \mu_1^2 \alpha_1} \sqrt{\sigma_2^2 + \mu_2^2 \alpha_2}} \quad (6)$$

Compared to the formula of the linear coefficient in Semeraro [20] the equation above has an additional parameter a that tunes the stochastic delay.

Finally, the *chf* of $\mathbf{Y}(t)$ is given by the following proposition.

Proposition 2.1. *Denote $\phi(u; \mu, \lambda)$ the *chf* of a rv distributed according to a $IG_T(\mu, \lambda)$ law then the joint *chf* at time t of $\mathbf{Y}(t)$ of Equation (4), where $H_j(t)$ and $I_j(t)$ are distributed as in (5) for $j = 1, 2$, is:*

$$\begin{aligned} \phi_{\mathbf{Y}(t)}(\mathbf{u}) = & \phi_{I_1(t)}\left(u_1 \mu_1 + i \frac{\sigma_1^2 u_1^2}{2}\right) \phi_{I_2(t)}\left(u_2 \mu_2 + i \frac{\sigma_2^2 u_2^2}{2}\right) \phi_{Z_a(t)}\left(u_2 \mu_2 + i \frac{\sigma_2^2 u_2^2}{2}\right) \\ & \phi_{H_1(t)}\left(\alpha_1 \left(u_1 \mu_1 + i \frac{\sigma_1^2 u_1^2}{2}\right) + a \alpha_2 \left(u_2 \mu_2 + i \frac{\sigma_2^2 u_2^2}{2}\right)\right) \end{aligned} \quad (7)$$

where

$$\begin{aligned} \phi_{H_j(t)}(u) &= \phi(u; At, A^2 t^2), \quad j = 1, 2 \\ \phi_{I_j(t)}(u) &= \phi(u; A_j t \gamma_j, A_j^2 t^2), \quad j = 1, 2 \\ \phi_{Z_a(t)}(u) &= \frac{\phi(u; At, A^2 t^2)}{\phi(au; At, A^2 t^2)} \end{aligned} \quad (8)$$

Proof. The proof follows the scheme we used to prove the Proposition 3.5 of Gardini et al. [11].

$I_j(t)$ and $H_1(t)$ are IG processes and hence their *chf*'s at time t can be computed starting from the *chf* expression of an IG rv, which is reported in Appendix A, whereas $Z_a(t)$ is the a -reminder of $H_1(t)$ and then its *chf* can be easily computed relying on Equation (1). The obtained *chf*'s of $H_j(t)$, $I_j(t)$ and $Z_a(t)$ are those of Equations (8).

Let be $\phi_{\mathbf{Y}(t)}(\mathbf{u}) := \mathbb{E}[e^{iu_1 Y_1(t) + iu_2 Y_2(t)}]$ the *chf* of the process $\mathbf{Y}(t)$ defined in (4): conditioning on $G_1(t)$ and $G_2(t)$ and recalling that $W_1(t)$ and $W_2(t)$ are independent BM's we get:

$$\phi_{\mathbf{Y}(t)}(\mathbf{u}) = \mathbb{E} \left[e^{i \left(u_1 \mu_1 + i \frac{\sigma_1^2 u_1^2}{2} \right) G_1(t)} e^{i \left(u_2 \mu_2 + i \frac{\sigma_2^2 u_2^2}{2} \right) G_2(t)} \right]$$

Substitute in the previous equation the expression of $G_j(t)$, given by (3), for $j = 1, 2$: by the property of the expected value for the product of independent rv 's, since $I_j(t)$, $H_1(t)$ and $Z_a(t)$ are mutually independent processes, we finally get the result of the Equation (7). \square

2.2 Semeraro-Luciano's sd -NIG model

In this subsection we extend the model of Luciano and Semeraro [14] and we build bivariate NIG processes with stochastic delays relying on the sd subordinators $(H_1(t), H_2(t))$ defined in (2). Unlike the previous model, standard correlated BM 's, $W_j^\rho(t)$, are considered in order to obtain higher correlations in log-returns.

Let $I_j(t)$, $j = 1, 2$, be subordinators and let $H_1(t)$ and $H_2(t)$ be two sd subordinators independent of $I_j(t)$. We define:

$$\mathbf{Y}^\rho(t) = \begin{pmatrix} \mu_1 I_1(t) + \sigma_1 W_1(I_1(t)) + \alpha_1 \mu_1 H_1(t) + \sqrt{\alpha_1} \sigma_1 W_1^\rho(H_1(t)) \\ \mu_2 I_2(t) + \sigma_2 W_2(I_2(t)) + \alpha_2 \mu_2 H_2(t) + \sqrt{\alpha_2} \sigma_2 (W_2^\rho(aH_1(t)) + \tilde{W}(Z_a(t))) \end{pmatrix} \quad (9)$$

where $W_1(t)$ and $W_2(t)$ are standard independent BM 's, $\mathbb{E}[dW_1^\rho(t) dW_2^\rho(t)] = \rho dt$ and $\tilde{W}(t)$ is another standard BM independent of $\mathbf{W}(t) = (W_1(t), W_2(t))$ and $\mathbf{W}^\rho(t) = (W_1^\rho(t), W_2^\rho(t))$.

A bivariate version of NIG process with sd -subordinators can be easily obtained letting $H_j(t)$ and $I_j(t)$ for $j = 1, 2$ be distributed as in the previous section. Moreover, the expression of the chf of the process $\mathbf{Y}^\rho(t)$ at time t is given by the following proposition.

Proposition 2.2. *The joint chf $\phi_{\mathbf{Y}^\rho(t)}(\mathbf{u})$ of the process $\mathbf{Y}^\rho(t) = (Y_1^\rho(t), Y_2^\rho(t))$ at time t defined in (9) is given by:*

$$\begin{aligned} \phi_{\mathbf{Y}(t)^\rho}(\mathbf{u}) = & \phi_{I_1(t)} \left(u_1 \mu_1 + \frac{i}{2} \sigma_1^2 u_1^2 \right) \phi_{I_2(t)} \left(u_2 \mu_2 + \frac{i}{2} \sigma_2^2 u_2^2 \right) \\ & \phi_{H_1(t)} \left(\frac{i}{2} u_1^2 \alpha_1 \sigma_1^2 (1-a) + \mathbf{u}^T \boldsymbol{\mu} + \frac{i}{2} \mathbf{u}^T a \Sigma \mathbf{u} \right) \phi_{Z_a(t)} \left(u_2 \mu_2 \alpha_2 + \frac{i}{2} u_2^2 \alpha_2 \sigma_2^2 \right) \end{aligned}$$

where $\boldsymbol{\mu} = [\alpha_1 \mu_1, a \alpha_2 \mu_2]$ and

$$\Sigma = \begin{bmatrix} \alpha_1 \sigma_1^2 & \sqrt{\alpha_1 \alpha_2} \sigma_1 \sigma_2 \rho \\ \sqrt{\alpha_1 \alpha_2} \sigma_1 \sigma_2 \rho & \alpha_2 \sigma_2^2 \end{bmatrix}$$

where $\phi_{H_1(t)}$, $\phi_{H_2(t)}$ and $\phi_{Z_a(t)}$ were defined in Proposition 2.1.

Proof. The proof retraces the idea we used in the proof of Proposition 2.1, recalling, in addition, that the *chf* $\varphi(\mathbf{t})$ of a multivariate normal *rv* with mean vector $\boldsymbol{\mu}$ and covariance matrix $\boldsymbol{\Sigma}$ is given by:

$$\varphi(\mathbf{t}) = \exp\left(i\boldsymbol{\mu}^T \mathbf{t} - \frac{1}{2}\mathbf{t}^T \boldsymbol{\Sigma} \mathbf{t}\right).$$

□

It is easy to show, by direct computation or by using the *chf* of Proposition 2.2, that the linear correlation coefficient at time t is given by:

$$\rho_{\mathbf{Y}^\rho(t)} = \frac{a(\mu_1\mu_2\alpha_1\alpha_2A + \rho A\sigma_1\sigma_2\sqrt{\alpha_1\alpha_2})}{\sqrt{\sigma_1^2 + \mu_1^2\alpha_1}\sqrt{\sigma_2^2 + \mu_2^2\alpha_2}} \quad (10)$$

Once again, a can be seen as the parameter that activates stochastic delay.

2.3 Ballotta-Bonfiglioli's *sd*-NIG model

The construction of bivariate Lévy processes proposed by Ballotta and Bonfiglioli [1] is slightly different from those of Semeraro [20] and Luciano and Semeraro [14] because the dependence is not introduced at the level of the subordinators but rather directly on the subordinated processes. Nevertheless, we can also extend this approach to include stochastic delay.

The construction of the a bivariate process with stochastic delay proceeds as follow. Let $H_1(t)$ and $H_2(t)$ be *sd* subordinators of (2): define subordinated *BM*'s $R_j(t)$, for $j = 1, 2$, with drift $\beta_{R_j} \in \mathbb{R}$ and diffusion $\gamma_{R_j} \in \mathbb{R}^+$, as:

$$\begin{aligned} R_1(t) &= \beta_{R_1}H_1(t) + \gamma_{R_1}W(H_1(t)) \\ R_2(t) &= \beta_{R_2}H_2(t) + \gamma_{R_2}\left(W(aH_1(t)) + \tilde{W}(Z_a(t))\right) \end{aligned} \quad (11)$$

where $W(t)$ and $\tilde{W}(t)$ are standard independent *BM*'s. Let subordinated *BM*'s $X_j(t)$, with drift $\beta_j \in \mathbb{R}$ and diffusion $\gamma_j \in \mathbb{R}^+$, be given by:

$$X_j(t) = \beta_j G_j(t) + \gamma_j W_j(G_j(t))$$

where $W_j(t)$ are standard independent *BM*'s whereas $G_j(t)$ are arbitrary subordinators with variance at time $t = 1$ given by $\nu_j \in \mathbb{R}^+$.

Finally, combining previous processes, we can define the process $\mathbf{Y}(t)$ as follow:

$$\mathbf{Y}(t) = (Y_1(t), Y_2(t)) = (X_1(t) + a_1 R_1(t), X_2(t) + a_2 R_2(t)) \quad (12)$$

where $a_j \in \mathbb{R}$.

As detailed in Ballotta and Bonfiglioli [1] and Gardini et al. [11], for any chosen distribution for the margin process $Y_j(t)$, for example a NIG distribution, it is possible to impose convolution conditions on processes $X_j(t)$ and $R_j(t)$ so that their linear combination has the same given distribution of $Y_j(t)$. The following proposition shows how to build a bivariate NIG process with stochastic delays and gives the closed form expression for its *chf*.

Proposition 2.3. *Consider an IG subordinator $H_1(t) \sim IG_T\left(t, \frac{t^2}{\nu_R}\right)$, $H_2(t)$ defined in Equation (2) and $R_j(t)$ given by (11). Let then $X_j(t)$ be a subordinated BM via an IG process $G_j(t) \sim IG_T\left(t, \frac{t^2}{\nu_j}\right)$, for $j = 1, 2$.*

*Then the components $Y_j(t)$ in (12) are distributed according to a NIG law and the joint *chf* is*

$$\phi_{\mathbf{Y}(t)}(u_1, u_2) = \phi\left(\beta_1 u_1 + \frac{i}{2} u_1^2 \gamma_1^2; t, \frac{t^2}{\nu_1}\right) \phi\left(\beta_2 u_2 + \frac{i}{2} u_2^2 \gamma_2^2; t, \frac{t^2}{\nu_2}\right) \xi(\mathbf{a} \circ \mathbf{u}) \quad (13)$$

where $\phi(u; \mu, \lambda)$ is the *chf* of a $IG_T(\mu, \lambda)$ distributed rv, $\mathbf{a} = (a_1, a_2)$, $\mathbf{u} = (u_1, u_2)$ and \circ is the Hadamard product. Finally $\xi(\mathbf{u})$ is given by:

$$\begin{aligned} \xi(\mathbf{w}) = & \phi\left(w_1 \beta_{R_1} + w_2 \beta_{R_2} a + \frac{i}{2} (w_1^2 \gamma_{R_1}^2 + 2w_1 w_2 \gamma_{R_1} \gamma_{R_2} a + w_2^2 a \gamma_{R_2}^2); t, \frac{t^2}{\nu_R}\right) \\ & \frac{\phi\left(w_2 \beta_{R_2} + \frac{i}{2} w_2^2 \gamma_{R_2}^2; t, \frac{t^2}{\nu_R}\right)}{\phi\left(w_2 a \beta_{R_2} + \frac{i}{2} a^2 w_2^2 \gamma_{R_2}^2; t, \frac{t^2}{\nu_R}\right)} \end{aligned} \quad (14)$$

Proof. Relying on properties of the IG distribution in Appendix A, it is easy to check that marginal distributions of $\mathbf{Y}(t)$ process have a NIG law.

Since $X_1(t)$, $X_2(t)$ and $\mathbf{R}(t)$ are mutually independent we have that

$$\phi_{\mathbf{Y}(t)}(u_1, u_2) = \mathbb{E}[e^{iu_1 X_1(t)}] \mathbb{E}[e^{iu_2 X_2(t)}] \mathbb{E}[e^{iu_1 R_1(t) + iu_2 R_2(t)}] \quad (15)$$

The computation consists in two steps: firstly we compute the *chf* $\mathbb{E}[e^{iu_1 R_1(t) + iu_2 R_2(t)}]$ of the joint process $\mathbf{R}(t)$ at time t defined in (11). This can be done by conditioning with respect $H_1(t)$ and $Z_a(t)$, relying upon the independence of $W(t)$ and $\tilde{W}(t)$ and recalling the expression of the *chf* of a $IG_T\left(t, \frac{t^2}{\nu_R}\right)$ rv, which is given in Appendix A, and that of its a -reminder, obtained by applying the Equation (1). By direct computation we obtain that the *chf* of $\mathbf{R}(t)$ has the form shown in Equation (14) valuated at $\mathbf{w} = \mathbf{a} \circ \mathbf{u}$.

Secondly, we observe that first two terms of the right hand side of the Equation (15) are the *chf*'s of subordinated BM's where subordinators are IG processes and hence their expressions are given by:

$$\mathbb{E}[e^{iu_j X_j(t)}] = \phi\left(\beta_j u_j + \frac{i}{2} u_j^2 \gamma_j^2; t, \frac{t^2}{\nu_j}\right) \quad (16)$$

where $\phi(u; \mu, \lambda)$ denotes the *chf* of a *rv* with $IG_T(\mu, \lambda)$ law. Combining Equations (14), (15) and (16) we finally obtain (13). \square

The linear correlation coefficient of a bivariate *sd*-NIG process at time t can be directly computed and it is given by:

$$\rho_{\mathbf{Y}(t)} = \frac{a_1 a_2 a (\beta_{R_1} \beta_{R_2} \nu_R + \gamma_{R_1} \gamma_{R_2})}{\sqrt{\sigma_1^2 + \mu_1^2 \alpha_1} \sqrt{\sigma_2^2 + \mu_2^2 \alpha_2}} \quad (17)$$

As expected, if $a = 1$ we retrieve the original expression of correlation coefficient obtained by Ballotta and Bonfiglioli [1].

3 Simulation Algorithm

Simulating the paths of the model dynamics defined in Section 2 can be accomplished by simulating BM's on a stochastic time grid generated by the relative IG *sd* subordinators. These subordinators are only marginally IG, in order to get the joint trajectories one has to simulate the skeleton of $Z_a(t)$ in (2) and therefore must have a way to draw from the law of the a -remainder Z_a of an IG distribution.

The methodology that we propose in this section is based on the close relation between *sd* laws and Lévy-driven OU processes. Following the naming convention in Barndorff-Nielsen and Shephard [4] we say that a Lévy-driven OU process $X(t)$ is a IG-OU process if its stationary law is an IG_B distribution with scale parameter δ and shape parameter γ . Now a well known result (see for instance Cont and Tankov [7] or Sato [19]) is that, a given one-dimensional distribution D always is the stationary law of a suitable Lévy-driven OU process if and only if D is *sd*. As shown by Halgreen [12] the IG law is *sd* and can be taken as the stationary distribution of a fully-fledged OU process.

We recall that a Lévy-driven OU process is defined as,

$$X(t) = X(0) e^{-\lambda t} + \int_0^t e^{-\lambda(t-u)} dL(u) \quad (18)$$

where $L(t)$ is a Lévy process and $\lambda > 0$. In addition, as observed in Barndorff-Nielsen and Shephard [4], $X(t)$ is stationary if and only if the *chf* $\phi_X(u)$ of its marginal distribution is of the form

$$\phi_X(u) = \phi_X(u e^{-\lambda t}) \chi_a(u, t)$$

where $\chi_a(u, t)$ is the *chf* of the second term of (18). On the other hand, due to the definition of *sd*, the last equation means that $\chi_a(u, t)$ is the *chf* of the a -remainder of the stationary law if one sets $a = e^{-\lambda t}$. We can then write

$$X(t) = X(0) e^{-\lambda t} + Z_{e^{-\lambda t}}(t). \quad (19)$$

Note that the parameter $e^{-\lambda t}$ is now time-dependent and the law of $Z_{e^{-\lambda t}}(t)$ coincides with that of $Z_a(t)$ with $a = e^{-\lambda t}$ only at a given time t , indeed $Z_{e^{-\lambda t}}(t)$ is not Lévy but rather an additive process. Nevertheless, in practice the simulation of the skeleton of a IG-OU process relies on the generation of a rv that is distributed according to the law of the a -remainder of the stationary distribution setting $a = e^{-\lambda t}$.

Starting from the results of Zhang and Zhang [23] relative to IG-OU processes, we derive an efficient algorithm to simulate the a -remainder of the $IG_B(\delta, \gamma)$, that is the building block for the generation of the trajectory of the process $Z_a(t)$.

Theorem 3.1 (Zhang and Zhang [23]). *The rv*

$$Z_a^\Delta = \int_0^\Delta e^{-\lambda(\Delta-u)} dL(u), \quad a = e^{-\lambda\Delta}, \quad \Delta > 0$$

can be represented as

$$Z_a^\Delta \stackrel{d}{=} W_0^\Delta + \sum_{i=1}^{\tilde{N}^\Delta} W_i^\Delta$$

where $W_0^\Delta \sim IG_B\left(\delta\left(1 - e^{-\frac{1}{2}\lambda\Delta}\right), \gamma\right)$, \tilde{N}^Δ is a Poisson-distributed rv with parameter $\delta\left(1 - e^{-\frac{1}{2}\lambda\Delta}\right)\gamma$ and W_i^Δ are independent rv 's with pdf:

$$f_{W^\Delta}(w) = \frac{\gamma^{-1}}{\sqrt{2\pi}} w^{-\frac{3}{2}} \left(e^{\frac{1}{2}\lambda\Delta} - 1\right)^{-1} \left(e^{-\frac{1}{2}\gamma^2 w} - e^{-\frac{1}{2}\gamma^2 w e^{\lambda\Delta}}\right) \mathbb{1}_{\{w>0\}}(w) \quad (20)$$

Assuming for simplicity $\Delta = 1$, we can then rely on Theorem 3.1 to conceive the simulation procedure of two correlated IG rv 's with linear correlation coefficient a and hence of the sd subordinators of (2) simply setting $\lambda = -\log a$. We get:

$$Z_a \stackrel{d}{=} W_0 + \sum_{i=1}^{\tilde{N}} W_i$$

where $W_0 \sim IG\left(\delta\left(1 - a^{\frac{1}{2}}\right), \gamma\right)$ and $\tilde{N} \sim Poisson\left(\delta\left(1 - a^{\frac{1}{2}}\right)\gamma\right)$.

Drawing from IG and Poisson laws is relatively easy, whereas the simulation of W_i is non-standard and can be generated using the acceptance-rejection algorithm proposed by Zhang and Zhang [23] observing that:

$$f_W(w) \leq c \cdot \Gamma\left(\frac{1}{2}, \frac{1}{2}\gamma^2\right)$$

where $c = \frac{1}{2}\left(1 + e^{\frac{1}{2}\lambda}\right)$ and $\Gamma(\alpha, \beta)$ denote the law of a gamma rv with shape $\alpha > 0$ and rate $\beta > 0$.

Although Zhang and Zhang [23] has illustrated a more accurate solution to reduce the expected number of iterations before acceptance c , acceptance-rejection algorithms might be slow and then sometimes inadequate for real time applications. This situation is exacerbated if the software implementation relies on interpreted languages like MATLAB, Python or R. In the following, we detail a simple and more efficient way to draw from the *pdf* $f_{W\Delta}(w)$ without relying on acceptance-rejection methods.

Assuming once again $\Delta = 1$ and $\lambda = -\log a$, equation (20) becomes:

$$f_W(w) = \frac{\gamma^{-1}}{\sqrt{2\pi}} w^{-\frac{3}{2}} \left(a^{-\frac{1}{2}} - 1\right)^{-1} \left(e^{-\frac{1}{2}\gamma^2 w} - e^{-\frac{1}{2}\gamma^2 \frac{w}{a}}\right) \mathbb{1}_{\{w>0\}}(w).$$

We recall that a *rv* is distributed according to a Gamma law with shape $\alpha > 0$ and rate $\beta > 0$ if its *pdf* is:

$$f(x) = \frac{\beta^\alpha}{\Gamma(\alpha)} x^{\alpha-1} e^{-\beta x}$$

where $\Gamma(z) = \int_0^\infty x^{z-1} e^{-x} dx$ is the Euler Gamma function. Knowing that $\Gamma(\frac{1}{2}) = \sqrt{\pi}$ and observing that:

$$\int_1^{\frac{1}{a}} e^{-\frac{\gamma^2}{2} w y} \frac{\gamma^2}{2} w dy = e^{-\frac{\gamma^2}{2} w} - e^{-\frac{\gamma^2}{2} \frac{w}{a}}$$

we can write:

$$\begin{aligned} f_W(w) &= \int_1^{\frac{1}{a}} \frac{y^{-\frac{1}{2}}}{2(a^{-\frac{1}{2}} - 1)} \cdot \frac{\left(\frac{\gamma^2}{2} y\right)^{\frac{1}{2}} w^{-\frac{1}{2}} e^{-\frac{\gamma^2}{2} y w}}{\Gamma(\frac{1}{2})} dy \\ &= \int_1^{\frac{1}{a}} f_Y(y) \cdot f_\Gamma\left(w \middle| \alpha = \frac{1}{2}, \beta = \frac{\gamma^2}{2} y\right) dy \end{aligned}$$

This means that $f_W(w)$ is a mixture of a Gamma law $\Gamma\left(\alpha = \frac{1}{2}, \beta = \frac{\gamma^2}{2} y\right)$ and a law whose *pdf* and *cdf* are respectively:

$$\begin{aligned} f_Y(y) &= \frac{y^{-\frac{1}{2}}}{2(a^{-\frac{1}{2}} - 1)} \mathbb{1}_{1 \leq y \leq \frac{1}{a}} \\ F_Y(y) &= \frac{y^{\frac{1}{2}} - 1}{a^{-\frac{1}{2}} - 1} \mathbb{1}_{1 \leq y \leq \frac{1}{a}} \end{aligned}$$

The simulation of Z_a and of the *rv* Y distributed according to the law with *cdf* $F_Y(y)$ is straightforward as is summarized in Algorithms 1 and 2, respectively.

Algorithm 1 Simulation of Z_a

- 1: Simulate $W_0 \sim IG(\delta(1 - \sqrt{a}), \gamma)$
 - 2: Simulate $\tilde{N} \sim Poisson(\delta(1 - \sqrt{a})\gamma)$
 - 3: Simulate $W_i, i = 1 \dots \tilde{N}$ using Algorithm 2
 - 4: Set $Z_a = \sum_{i=0}^{\tilde{N}} W_i$
-

Algorithm 2 Simulation of W_i, \tilde{N}

- 1: Simulate $U_i \sim U([0, 1])$
 - 2: Compute $Y_i = \left(1 + \left(a^{-\frac{1}{2}} - 1\right)U_i\right)^2$
 - 3: Simulate W_i from a $\Gamma\left(\frac{1}{2}, \frac{1}{2}\gamma^2 Y_i\right)$
-

In Table 1 we compare theoretical values of the first five moments of Z_a against those obtained by MC simulations using Algorithm 1. We observe that the precision of the algorithms is good for different values of $a \in (0, 1)$. In Figure 2 we draw the probability density function of two correlated *rv* $X, Y \sim IG_B(\delta, \gamma)$ and their scatter plot for two different values of a .

The proposed algorithm is extremely fast as one can see from results reported in Table 2. This time complexity analysis was implemented on a PC having an Intel Core i5-10210U 2.11 GHz processor.

The simulation of the a -remainder of an IG law provides the generation of the joint trajectories of the *sd* subordinators $H_1(t), H_2(t)$ and therefore of the models presented in Section 2. The application of these MC schemes will be shown in next section.

4 Financial Application

In this section we use the bivariate Lévy processes illustrated in Section 2 to model power and gas forward markets.

Following Cont and Tankov [7], we assume that each forward price dynamics is driven by an exponential Lévy process based on $Y_j(t), j = 1, 2$ derived in Section 2. The forward price $F_j(t), j = 1, 2$ at time t can be defined as follow:

$$F_j(t) = F_j(0) e^{\omega_j t + Y_j(t)} \quad (21)$$

where ω_j is the drift correction required for risk-neutral arguments such that

$$\omega_j = -\varphi_j(-i) \quad (22)$$

where $\varphi_j(u)$ is the characteristic exponent of the process $Y_j(t)$.

$\mathbb{E}[Z_a^n]$	T	N
$\mathbb{E}[Z_a^1]$	3.00	3.00
$\mathbb{E}[Z_a^2]$	10.47	10.48
$\mathbb{E}[Z_a^3]$	42.17	42.26
$\mathbb{E}[Z_a^4]$	194.72	195.49
$\mathbb{E}[Z_a^5]$	1021.84	1029.41

(a) $a = 0.1$

$\mathbb{E}[Z_a^n]$	T	N
$\mathbb{E}[Z_a^1]$	1.00	1.00
$\mathbb{E}[Z_a^2]$	1.76	1.76
$\mathbb{E}[Z_a^3]$	4.56	4.59
$\mathbb{E}[Z_a^4]$	15.77	15.89
$\mathbb{E}[Z_a^5]$	67.94	68.66

(c) $a = 0.7$

$\mathbb{E}[Z_a^n]$	T	N
$\mathbb{E}[Z_a^1]$	1.67	1.67
$\mathbb{E}[Z_a^2]$	3.89	3.89
$\mathbb{E}[Z_a^3]$	11.91	11.90
$\mathbb{E}[Z_a^4]$	45.58	45.46
$\mathbb{E}[Z_a^5]$	209.90	208.97

(b) $a = 0.5$

$\mathbb{E}[Z_a^n]$	T	N
$\mathbb{E}[Z_a^1]$	0.33	0.33
$\mathbb{E}[Z_a^2]$	0.39	0.40
$\mathbb{E}[Z_a^3]$	0.85	0.86
$\mathbb{E}[Z_a^4]$	2.66	2.68
$\mathbb{E}[Z_a^5]$	10.71	10.72

(d) $a = 0.9$

Table 1: Moments comparison using $N_{sim} = 10^6$ for $\delta = 5$ and $\gamma = 1.5$. T stands for the values of the theoretical n-th moment, whereas N stands for the MC-based estimations.

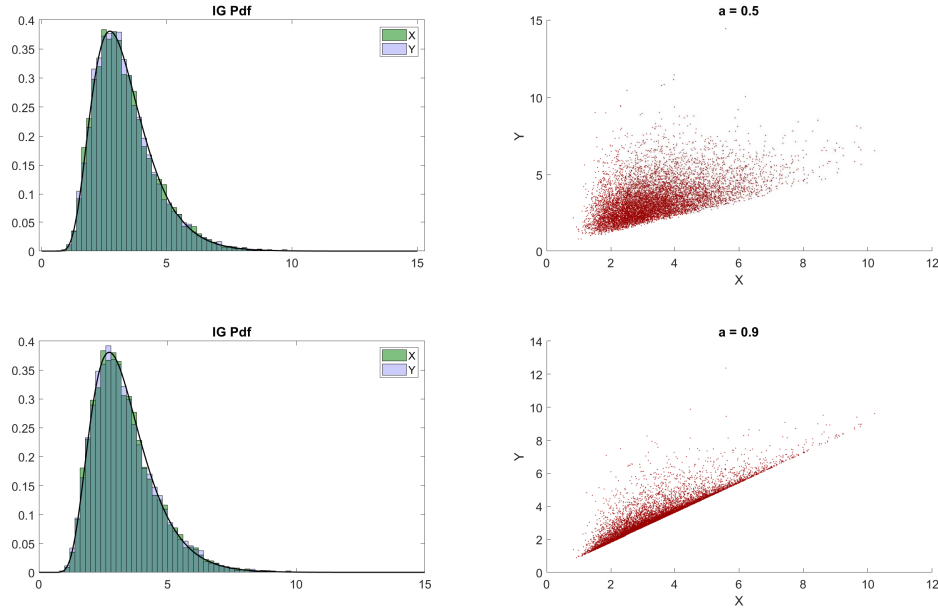


Figure 2: Correlated rv X and Y for $\delta = 5$ and $\gamma = 1.5$ and their scatter plots for $a = 0.5$ and $a = 0.9$.

N_{sim}	10^3	10^4	10^5	10^6
Time (s)	$1.05 \cdot 10^{-5}$	$6.54 \cdot 10^{-5}$	$6.98 \cdot 10^{-4}$	$7.48 \cdot 10^{-3}$

Table 2: Average computational time on one hundred runs of Algorithm 2 varying the number of simulations.

In order to calibrate our model we use the two steps procedure adopted in Luciano and Semeraro [14] and in Gardini et al. [11]: since the marginal distributions do not depend on the parameters used to model the structure of dependence one can firstly fit the marginal parameters on quoted vanilla product and, secondly, dependence ones on forward historical data. The choice of fitting the dependence structure on historical quotations is motivated by the fact that derivative contracts written on more than one underlying asset are extremely illiquid.

Once calibrated the marginal parameters, we consider spread options written on future prices, which payoff is given by

$$\Phi_T = (F_1(T) - F_2(T) - K)^+$$

can be priced. It customary to reserve the name *Cross-Border* or *Spark-Spread* option if the futures are relative to power or gas markets, respectively. In all experiments we use the MC technique with $N_{sim} = 10^6$ simulations and the Fourier-based method presented by Caldana and Fusai [6]. This method provides a good approximation for spread-options prices and it's simpler to implement than the one proposed by Hurd and Zhou [13], because it requires only one Fourier inversion.

The numerical investigation is split into two parts: in the first one we use *sd*-NIG processes to model German and French power forward markets, whereas in the second part we focus on German power and natural gas forward markets.

All these markets are very correlated in particular, the German and French power forward markets exhibit an extremely high log-returns correlation. This is due to the structure of the electricity network that connects the two countries and to the fact that electricity cannot be stored. Therefore, if the price of electricity rises in Germany we can observe an increase of electricity prices in French as well. The log-returns correlation between German power and natural gas forward markets is still positive but lower than that of the previous case. This depends on the percentage of installed capacity depending on natural gas (in 2020, 13.9% in Germany) and, moreover, gas can be stored. For the sake of concision we introduce the following notation:

- (*SSD* - *NIG*): *sd*-NIG model presented in Section 2.1.
- (*LSSD* - *NIG*): *sd*-NIG model presented in Section 2.2.
- (*BBSD* - *NIG*): *sd*-NIG model presented in Section 2.3.

4.1 Application to German and French Power Markets

In order to calibrate the proposed *sd*-NIG models we rely upon derivative contracts written on the forward price of each underlying and upon the joint historical time series of forward quotations. The data-set¹ is composed as follow:

- Forward quotations from 25 April 2017 to 12 November 2018 of Calendar 2019 power forward. Calendar power forward in German and France are stated respectively with DEBY and F7BY.
- Call Options on power forward 2019 quotations for both countries with settlement date 12 November 2018. We used strikes in a range of ± 10 [EUR/MWh] around the settlement price of the forward contract.
- We assume a risk-free rate $r = 0.015$.
- The historical correlation observed between markets is $\rho_{mkt} = 0.94$.

We denote (θ_1, θ_2) parameters related to the French and German power forward markets respectively. Defining the error ϵ_i as

$$\epsilon_i = \frac{C_i^\theta(K, T) - C_i}{C_i},$$

where $C_i^\theta(K, T)$ is the value of the i -th Call option obtained by the model and C_i is its market price, the picture at the bottom of Figure 3 shows that all models provide a good fit for quoted market options because ϵ is negligible. In Figure 3 the picture at the top shows that the *SSD-NIG* model overprices *Cross-Border* options: this is because the fitted model correlation is low, as shown by the value ρ_{mod} in Table 4, so one should avoid using this model for pricing. For *LSSD-NIG* model the situation is better but it is not really able to capture the prevailing market correlation. Fortunately *BBSD-NIG* model can replicate the market correlation and then can be used to price *Cross-Border* options. Fitted common parameters are shown in Table 3, whereas the dependence parameters for *SSD-NIG*, *LSSD-NIG* and *BBSD-NIG* models are shown in Tables 4, 5, 6, respectively. The value of a , is shown in Table 7. We observe that the parameter a is very close to one, as one should expected. Indeed this result has a very natural economic interpretation: the European electricity network is strongly connected and a price movement in either the German or French market one is propagated without stochastic delay. Finally, in Table 8 we compare values of *Cross-Border* options priced using the FFT method proposed by Caldana and Fusai [6] and the MC scheme we proposed in Section 3. Option prices provided by both algorithms are very close and this allows us to use indistinctly FFT or MC method.

¹Data Source: www.eex.com.

Model	μ_1	μ_2	σ_1	σ_2	α_1	α_2
<i>SSD</i>	0.64	0.40	0.31	0.32	0.02	0.03
<i>LSSD</i>	0.64	0.40	0.31	0.32	0.02	0.03
<i>BBSD</i>	0.64	0.40	0.31	0.32	0.02	0.03

Table 3: Fitted marginal parameters for German and French power markets.

Parameter	Value
<i>A</i>	40.15
<i>B</i>	1.00
<i>a</i>	0.99
ρ_{mod}	0.05

Table 4: *SSD*

Parameter	Value
<i>A</i>	40.15
<i>B</i>	1.00
ρ	0.99
<i>a</i>	0.99
ρ_{mod}	0.88

Table 5: *LSSD*

Parameter	Value	Parameter	Value
β_1	-0.001	β_{R_2}	0.800
β_2	0.013	γ_{R_1}	0.448
γ_1	0.002	γ_{R_2}	0.50
γ_2	0.103	ν_R	0.025
ν_1	1.007	<i>a</i>	0.99
ν_2	0.091	ρ_{mod}	0.94
β_{R_1}	0.554		

Table 6: *BBSD*

Model	<i>a</i>
<i>SSD</i>	0.99
<i>LSSD</i>	0.99
<i>BBSD</i>	0.99

Table 7: Values for the *a* parameter of the three models.

4.2 Application to German Power market and NCG Gas Market

In this section we present numerical results obtained applying our models to German power forward market (DE) and to natural gas forward market (NCG). These two markets are positively correlated, but the log-return correlation is lower than the one between power futures.

The data-set² we relied upon is the following one:

- Forward quotations from 1 July 2019 to 09 September 2019 relative to the Month January 2020 for the Power Forward in Germany and the Gas NCG Forward.
- Call Options on power forward NCG with settlement date 9 September 2019. As done before, we use strike prices K in a range of ± 10 [EUR/MWh] around the settlement price of the forward contract.
- We assume a risk-free rate $r = 0.015$.
- The historical correlation between log-returns is $\rho_{mkt} = 0.54$.

²Data Source: www.eex.com and www.theice.com

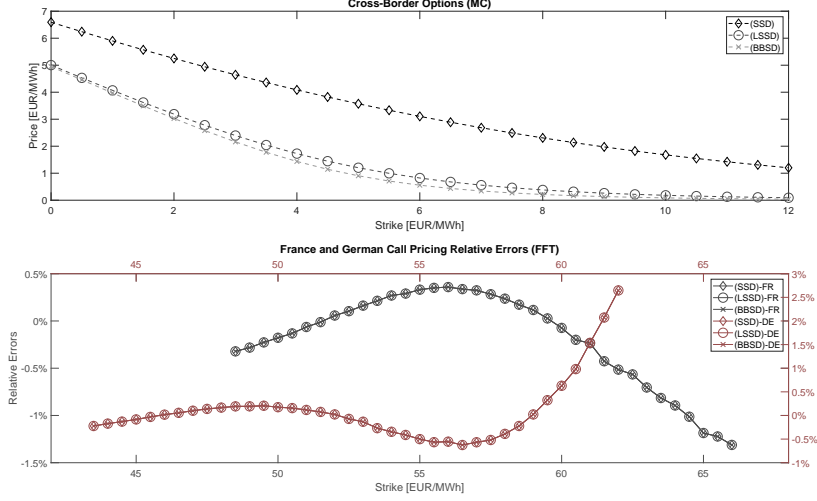


Figure 3: Percentage errors and Cross Border option prices.

In the picture at the bottom of Figure 4 we observe that all models provide a good fitting of quoted market options because the relative error ϵ_i is small. The picture at the top of Figure 4 shows that the *SSD-NIG* model overprices the Spark-Spread option due to the fact that fitted model correlation is close to zero, as shown by the value ρ_{mod} in Table 10. In contrast, *LSSD-NIG* and *BBSD-NIG* models provide a lower price and catch the right level of market correlation as shown in Tables 11,12. We can conclude that both *LSSD-NIG* and *BBSD-NIG* models can be used to price *Spark-Spread* options. Table 9 shows fitted common parameters whereas dependence parameters for *SSD-NIG*, *LSSD-NIG* and *BBSD-NIG* models are shown in Tables 10, 11, 12: the value of a , the sd parameter which aims to model the *stochastic delay*, is shown in Table 13. The value is still close to one but it is smaller than that estimated for the power forward markets. From the expressions of the linear correlation coefficient reported in equations (6), (10) and (17), it is easy to see that a change in the value of a has an impact on the value of the correlation coefficient and it is a matter of fact that even a small change in correlation has a high impact on the spread option price. On the other hand, unlike electricity, natural gas can be stored and therefore the impact on the power market can be moderated and delayed, for example, using storage contracts or other types of OTC derivatives. If the gas price suddenly rises then it is not rare to observe that electricity price is not immediately effected.

5 Conclusions

Using the concept of self-decomposable subordinators introduced by Gardini et al. [11], we have shown how some recently proposed multivariate Lévy models can be easily extended to include what we called *synaptic risk*. Based on this machinery,

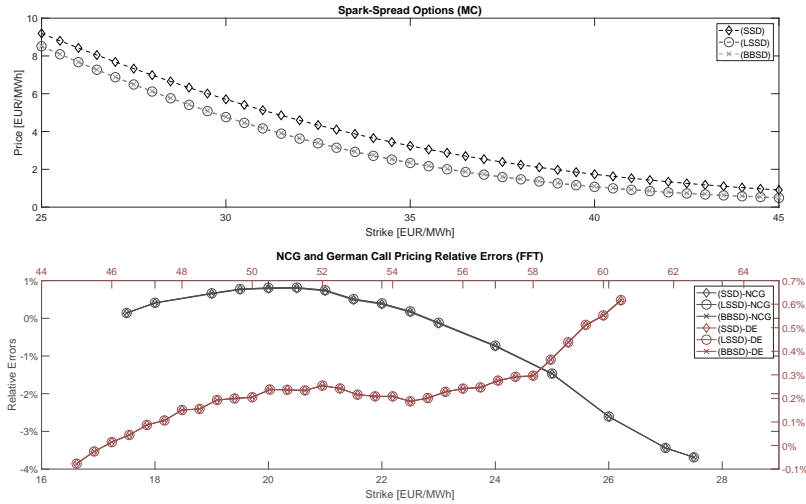


Figure 4: Percentage errors and Spark-Spread option prices.

we build new bivariate versions of a Normal Inverse Gaussian process aiming at capturing stochastic delays. Their mathematical tractability were preserved and, moreover, we derived closed form expressions for their characteristic functions and linear correlation coefficients. These results were instrumental to apply calibration and derivative pricing methods based on Fourier techniques.

Nevertheless, in many real applications, Monte Carlo simulations are required for complex derivative contracts pricing. Basing on some observations in Taufer and Leonenko [21] and Cufaro Petroni and Sabino [10] about the strong mathematical connection between self-decomposable laws and Lévy-driven Ornstein-Uhlenbeck processes, we developed a new efficient algorithm to generate the α -remainder of Inverse Gaussian law and hence to simulate the desired Normal Inverse Gaussian process with stochastic delays. The just mentioned algorithm is more efficient than the one proposed by Zhang and Zhang [23], because it is not based on acceptance-rejection methods: for this reason it can be adopted for real time simulations and pricing.

Eventually, we applied these results to the modeling of energy markets: using the two-steps calibration technique proposed by Luciano and Semeraro [14], all presented models have been calibrated on vanilla products and on historical quotations and, finally, commonly traded derivative contracts, such as *Cross-Border* or *Spark-Spread* options, have been efficiently priced using both Monte Carlo simulations and the Fourier method proposed by Caldana and Fusai [6].

In this article, we did not give a complete characterization of the Lévy process which can be built starting from the α -remainder of a self-decomposable law. For this reason it might be worth deeply investigating mathematical properties of such a process and those of the one obtained subordinating a standard Brownian Motion with it.

It is a well known fact that Inverse Gaussian and Gamma laws are special cases

of Generalized Inverse Gaussian laws which are self-decomposable, as was shown by Halgreen [12]. Zhang [22] gave a complete characterization of Ornstein-Uhlenbeck processes with Generalized Inverse Gaussian stationary laws: their numerical simulations, achieved by extending our new aforementioned approach, might be the object of a future research.

Many exotic derivatives widely traded in energy markets, such as swing and storage contracts, require Least Squares Monte Carlo approach in order to be valued: time reversal simulations approach presented in Pellegrino and Sabino [16] and Sabino [17] might be adapted to simulate backward in time above mentioned processes leading to efficient pricing algorithms: therefore, this topic will be the subject of future inquiries.

K	<i>SSD-NIG</i>			<i>LSSD-NIG</i>			<i>BBSD-NIG</i>		
-	FFT	MC	Δ	FFT	MC	Δ	FFT	MC	Δ
0.0	6.61	6.59	(0.02)	5.01	5.00	(0.01)	4.95	4.95	(0.00)
0.5	6.26	6.24	(0.02)	4.54	4.53	(0.01)	4.46	4.46	(0.00)
1.0	5.92	5.90	(0.02)	4.08	4.07	(0.01)	3.98	3.97	(0.01)
1.5	5.59	5.57	(0.02)	3.63	3.62	(0.01)	3.50	3.49	(0.01)
2.0	5.27	5.25	(0.02)	3.20	3.19	(0.01)	3.03	3.03	(0.00)
2.5	4.96	4.94	(0.02)	2.79	2.78	(0.01)	2.58	2.58	(0.00)
3.0	4.67	4.65	(0.02)	2.41	2.40	(0.01)	2.16	2.16	(0.00)
3.5	4.38	4.36	(0.02)	2.06	2.04	(0.02)	1.78	1.78	(0.00)
4.0	4.11	4.09	(0.02)	1.74	1.73	(0.01)	1.44	1.44	(0.00)
4.5	3.85	3.82	(0.03)	1.46	1.45	(0.01)	1.15	1.15	(0.00)
5.0	3.59	3.57	(0.02)	1.22	1.20	(0.02)	0.91	0.90	(0.01)
5.5	3.36	3.33	(0.03)	1.01	1.00	(0.01)	0.71	0.71	(0.00)
6.0	3.13	3.11	(0.02)	0.83	0.82	(0.01)	0.56	0.56	(0.00)
6.5	2.91	2.89	(0.02)	0.69	0.68	(0.01)	0.44	0.44	(0.00)
7.0	2.71	2.68	(0.03)	0.57	0.56	(0.01)	0.34	0.34	(0.00)
7.5	2.51	2.49	(0.02)	0.47	0.46	(0.01)	0.27	0.27	(0.00)
8.0	2.33	2.31	(0.02)	0.39	0.38	(0.01)	0.21	0.21	(0.00)
8.5	2.16	2.14	(0.02)	0.32	0.32	(0.00)	0.17	0.17	(0.00)
9.0	2.00	1.97	(0.03)	0.27	0.26	(0.01)	0.14	0.13	(0.01)
9.5	1.84	1.82	(0.02)	0.22	0.22	(0.00)	0.11	0.11	(0.00)
10.0	1.70	1.68	(0.02)	0.19	0.18	(0.01)	0.09	0.09	(0.00)
10.5	1.57	1.55	(0.02)	0.16	0.15	(0.01)	0.07	0.07	(0.00)
11.0	1.44	1.42	(0.02)	0.13	0.13	(0.00)	0.06	0.06	(0.00)
11.5	1.33	1.31	(0.02)	0.11	0.11	(0.00)	0.05	0.05	(0.00)
12.0	1.22	1.20	(0.02)	0.09	0.09	(0.00)	0.04	0.04	(0.00)

Table 8: Cross Border Option prices comparison between three models. Option prices are obtained using both FFT and MC methods. Δ is the difference between prices.

Model	μ_1	μ_2	σ_1	σ_2	α_1	α_2
<i>SSD</i>	0.37	0.20	0.44	0.33	0.09	0.07
<i>LSSD</i>	0.37	0.20	0.44	0.33	0.09	0.07
<i>BBSD</i>	0.37	0.20	0.44	0.33	0.09	0.07

Table 9: Fitted marginal parameters for German and French power markets.

Parameter	Value
A	11.27
B	1.00
a	0.99
ρ_{mod}	0.03

Table 10: *SSD*

Parameter	Value
A	8.79
B	1.00
ρ	0.87
a	0.90
ρ_{mod}	0.54

Table 11: *LSSD*

Parameter	Value	Parameter	Value
β_1	0.11	β_{R_2}	0.23
β_2	0.09	γ_{R_1}	0.56
γ_1	0.24	γ_{R_2}	0.50
γ_2	0.22	ν_R	0.13
ν_1	0.28	a	0.89
ν_2	0.15	ρ_{mod}	0.54
β_{R_1}	0.38		

Table 12: *BBSD*

Model	a
<i>SSD</i>	0.99
<i>LSSD</i>	0.90
<i>BBSD</i>	0.89

Table 13: Values for the a parameter of three models.

A IG laws parametrization

The characterization of the *pdf* of an IG law is not unique. For example, Cont and Tankov [7] proposed a parameters setting in (μ, λ) , that we denoted by $IG_T(\mu, \lambda)$ where $\mu > 0$ is the mean and $\lambda > 0$ is the shape parameter. Within this setting the *pdf* of an Inverse Gaussian law is given by:

$$f_Z(x; \mu, \lambda) = \left(\frac{\lambda}{2\pi x^3} \right)^{1/2} \exp \left\{ -\frac{\lambda(x - \mu)^2}{2\mu^2 x} \right\} \quad (23)$$

and its *chf* is:

$$\phi_Z(u) = \exp \left\{ \frac{\lambda}{\mu} \left[1 - \sqrt{1 - \frac{2iu\mu^2}{\lambda}} \right] \right\} \quad (24)$$

Moreover let be $X \sim IG_T(\mu, \lambda)$ then we have that:

$$\mathbb{E}[X] = \mu, \quad Var[X] = \frac{\mu^3}{\lambda}$$

The original parameter setting of a IG law proposed by Barndorff-Nielsen [2] is denoted with $IG_B(a, b)$, where a can be the scale parameter and b represents the shape of the distribution. Its probability density function is given by:

$$f_Z(x; a, b) = \frac{a}{\sqrt{2\pi}} \exp(ab) x^{-3/2} \exp \left(-\frac{1}{2} (a^2 x^{-1} + b^2 x) \right) \quad (25)$$

and the *chf* has the following form:

$$\phi_Z(u) = \exp \left\{ -a \left(\sqrt{-2iu + b^2} - b \right) \right\} \quad (26)$$

If $X \sim IG_B(a, b)$ then we have that:

$$\mathbb{E}[X] = \frac{a}{b}, \quad Var[X] = \frac{a}{b^3}$$

Both parametrizations can be adopted and it is possible to switch from one the other by observing that:

$$\mu = \frac{a}{b} \quad (27)$$

$$\lambda = a^2 \quad (28)$$

We report some very useful properties of the IG law.

- Let be $X \sim IG_B(a_1, b)$ and $Y \sim IG_B(a_2, b)$ and let X and Y be independent. Then:

$$cX \sim IG_B \left(ca_1, \frac{b}{c} \right), \quad X + Y \sim IG_B(a_1 + a_2, b)$$

- Let be $X \sim IG_T(\mu_0 w_1, \lambda_0 w_1^2)$ and $Y \sim IG_T(\mu_0 w_2, \lambda_0 w_2^2)$ and let X and Y be independent. Then:

$$cX \sim IG_T(c\mu_0 w_1, c\lambda_0 w_1), \quad X + Y \sim IG_T(\mu_0 (w_1 + w_2), \lambda_0 (w_1 + w_2)^2)$$

References

- [1] L. Ballotta and E. Bonfiglioli. Multivariate Asset Models Using Lévy Processes and Applications. *The European Journal of Finance*, 13(22):1320–1350, 2013.
- [2] O.E. Barndorff-Nielsen. Normal Inverse Gaussian Distributions and Stochastic Volatility Modelling. *Scandinavian Journal of Statistics*, 24(1):1–13, 1997.
- [3] O.E. Barndorff-Nielsen. Processes of Normal Inverse Gaussian Type. *Finance and Stochastics*, 2(1):41–68, 1998.
- [4] O.E. Barndorff-Nielsen and N. Shephard. Non-Gaussian Ornstein-Uhlenbeck-based models and some of their uses in financial economics. *Journal of the Royal Statistical Society: Series B*, 63(2):167–241, 2001.
- [5] F. Black and M. Scholes. The Pricing of Options and Corporate Liabilities. *Journal of Political Economy*, 81(3):637–654, 1973.
- [6] R. Caldana and G. Fusai. A General Closed-Form Spread Option Pricing Formula. *Journal of Banking & Finance*, 12(37):4863–4906, 2016.
- [7] R. Cont and P. Tankov. *Financial Modelling with Jump Processes*. Chapman and Hall, 2003.
- [8] N. Cufaro Petroni. Self-decomposability and Self-similarity: a Concise Primer. *Physica A, Statistical Mechanics and its Applications*, 387(7-9):1875–1894, 2008.
- [9] N. Cufaro Petroni and P. Sabino. Pricing Exchange Options with Correlated Jump Diffusion Processes. *Quantitative Finance*, 0(0):1–13, 2018.
- [10] N. Cufaro Petroni and P. Sabino. Gamma Related Ornstein–Uhlenbeck Processes and their Simulation. Forthcoming in *Journal of Statistical Computation and Simulation*, 2020.
- [11] M. Gardini, P. Sabino, and E. Sasso. Correlating Lévy Processes with Self-Decomposability: Applications to Energy Markets. 2020.
- [12] C. Halgreen. Self-decomposability of the Generalized Inverse Gaussian and Hyperbolic Distributions. *Zeitschrift für Wahrscheinlichkeitstheorie und Verwandte Gebiete*, 47(1):1432–2064, 1979.
- [13] T.R. Hurd and Z. Zhou. A Fourier Transform Method for Spread Option Pricing. <https://arxiv.org/pdf/0902.3643.pdf>, 2009.
- [14] E. Luciano and P. Semeraro. Multivariate Time Changes for Lévy Asset Models: Characterization and Calibration. *Journal of Computational and Applied Mathematics*, 233(1):1937–1953, 2010.

- [15] D. B. Madan and E. Seneta. The Variance Gamma (V.G.) Model for Share Market Returns. *The Journal of Business*, 63(4):511–524, 1990.
- [16] T. Pellegrino and P. Sabino. Enhancing Least Squares Monte Carlo with Diffusion Bridges: an Application to Energy Facilities. *Quantitative Finance*, 15(5):761–772, 2015.
- [17] P. Sabino. Forward or Backward Simulation? A Comparative Study. *Quantitative Finance*, 20(7):1213–1226, 2020. doi: 10.1080/14697688.2020.1741668.
- [18] P. Sabino. Exact Simulation of Variance Gamma-Related OU Processes: Application to the Pricing of Energy Derivatives. *Applied Mathematical Finance*, 0(0):1–21, 2020. doi: 10.1080/1350486X.2020.1813040.
- [19] K. Sato. *Lévy Processes and Infinitely Divisible Distributions*. Cambridge U.P., Cambridge, 1999.
- [20] P. Semeraro. A Multivariate Variance Gamma Model For Financial Applications. *International Journal of Theoretical and Applied Finance*, 11(1):1–18, 2008.
- [21] E. Taufer and N. Leonenko. Simulation of Lévy-driven Ornstein–Uhlenbeck Processes with Given Marginal Distribution. *Computational Statistics & Data Analysis*, 53(6):2427 – 2437, 2009. The Fourth Special Issue on Computational Econometrics.
- [22] S. Zhang. Transition Law-Based Simulation of Generalized Inverse Gaussian Ornstein–Uhlenbeck Processes. *Methodology and Computing in Applied Probability*, 13:619–656, 2011.
- [23] S. Zhang and X. Zhang. Exact Simulation of IG-OU Processes. *Methodology and Computing in Applied Probability*, 10(4):337–355, 2008.